Surface & Coatings Technology

Online publication complete: 27-NOV-2014

http://dx.doi.org/10.1016/j.surfcoat.2014.11.032

The chemical resistance of nano-sized SiC rich composite coating.

S. Gurbán, L. Kotis, A. Pongracz, A. Sulyok, A. L. Tóth, E. Vázsonyi, M. Menyhard

Institute for Technical Physics and Materials Science, Research Centre for Natural Sciences, Hungarian Academy of Sciences, 1121 Budapest, Konkoly Thege M. út 29-33

Abstract

30 keV Ga^+ implantation was applied to a nominally C(20 nm)/Si(20 nm)/C(20 nm)/Si(20 nm)/ C(20 nm)/Si substrate multilayer system. Due to the irradiation intermixing occurred and a layer containing C, Si, Ga and (amorphous) SiC was obtained. The thickness (7-30 nm) and composition of the layer depended on the fluence of irradiation. The chemical resistance of the layer was tested by applying microwave oxidation and various polysilicon etchants and was found to be excellent if the SiC concentration was above 20 %. Using etchant with etching rate of about 100 nm/s for poly-Si during 10 s had not affected the integrity of the intermixed region with a thickness of 10 nm only some defects appeared. With further increase of the etching time the size of defects increased resulting in inhomogeneous layer removal. The in-depth composition of non-defective region remained on the surface was determined by AES depth

profiling, which revealed that the intermixed layer did not change during the harsh etching except the removal of its thin surface layer containing less than 20% SiC. The etching rate of the intermixed layer is orders of magnitude lower than that for poly-Si.

*Corresponding author. E-mail: menyhard.miklos@ttk.mta.hu (Miklos Menyhard),
Tel: 36-306001063

1. Introduction

Recent technologies frequently apply nano-layers, nano-devices, etc. because of their exceptionally favorable characteristics. These devices might need coating layers to protect them from mechanical, chemical, biological attacks. The coating layers are generally made of high stability compounds with high heat of formation. To make such a compound, a high temperature process is usually applied; however the nano-devices generally cannot withstand such conditions. Thus, one should look for coating procedures which do not apply high temperature. Among others, ion bombardment induced mixing (shortly ion mixing) is such a process, which can be used for producing compounds of high heat of formation - at room temperature [1-5].

One of the widely used coating materials is SiC, a high band gap semiconductor which is also a high strength ceramics. Most of its applications are connected to its good resistance against temperature and chemical effects. Its chemical resistance is exceptional; a good quality SiC single crystal resists against nearly all aqueous etching solutions except phosphoric acid and various alkaline solutions at higher temperatures [6]. This excellent chemical resistance drops with the appearance of structural defects. E.g. SiC damaged by ion bombardment can be etched by 1unit volume HF+1 unit volume HNO_3 solution [7]. Similarly, amorphous SiC can also be "easily" etched [8], but the etching rate compared with "usual" materials is still low. Thus, the chemical resistance of the even imperfect SiC is high enough for various applications, such as improvement of the oxidation resistance of a carbon/carbon composite [9]. 250 nm thick amorphous SiC thin films proved to be excellent coating to protect the metallization of sensors working in harsh environment [10]. 50 nm thick polycrystalline SiC layer was used to improve the wear resistance of polycrystalline silicon micro-electro-mechanical system [11]. It has also

been shown that not only the SiC layer but composite layer containing SiC particles can be also used to improve the chemical resistance of a coating layer; improved corrosion resistance was found by introducing SiC-particles to electrolytic nickel layer [12,13]. It has been also shown that the corrosion resistance of Ni–Co/SiC nano composite coatings depends on the size of SiC particles; it was much better if SiC nano particles were used than in case if the composite contained micro sized SiC [14].

Thus, layers containing various kinds of SiC in varying amounts are useful protective coatings. The question arises, how much the thickness of the coating layer can be reduced while maintaining the sufficient chemical resistance.

We have shown that SiC rich nano layers in the range of 5-20 nm can be produced by ion mixing of C and Si layers [15]. The thickness and composition of the ion mixed layer can be tailored by changing the fluence and/or energy of the irradiation. Additional advantage of the method is that the layer can be produced according to any desired template if focused ion beam is applied for ion mixing. On the other hand these layers are far from being perfect SiC. Rather, they are layers containing most likely defective amorphous SiC together with other components like C, Si and Ga. Based on the literature [12-14] one might hope that even such layers have high (compared to "usual" materials) resistance against chemical attack. Thus, we have studied the chemical resistance of these layers as a function of their thickness. We will show that the etching rates applying usual aqueous etching solutions of these only some nanometer thick layers, containing less than 100 % amorphous SiC, are orders of magnitude less than that of poly-Si.

2. Experimental

2.1. Producing SiC rich layer

C /Si /C /Si /C /Si single crystal substrate multilayered specimen was produced by magnetron sputtering. The structures of the actual specimens were determined by cross sectional transmission electron microscopy (XTEM) as: 1^{st} C 20 nm / 1^{st} Si 20 nm / 2^{nd} C 19 nm / 2^{nd} Si 23 nm /3^{rd} C 18 nm / Si substrate. The layers are counted from the top surface. The silicon and carbon layers were polycrystalline and amorphous, respectively [15].

To make the SiC rich layer the specimen was irradiated by Ga^+ ions using LEO 1540XB (FEG SEM – FIB) cross beam system at room temperature. The angle of incidence of the ion bombardment was 0^o (with respect the surface normal). The energy of the Ga^+ projectiles was 30 keV, and the applied fluences of 10, 20, 40, 80, 120 x 10^{15} Ga^+/cm^2 were determined by the time of the single pass irradiation. The ion current density was some nA/mm^2 and thus the heating effects and/or overlapping of cascades could be neglected. The irradiated areas varied from 100μm x100μm to 300μm x300μm.

2.2. AES depth profiling

To determine the depth profiles at various stages of the experiment (as received, after ion beam mixing, after various etching) Auger Electron Spectroscopy (AES) depth profiling was applied.

2.2.1. Sputter removal

1 keV Ar^+ ions with angle of incidence of 80^o (with respect to the surface normal) were used for depth profiling. The ion beam was scanned; the sputtering rate on an area of 1.5x1.8 mm^2 was uniform. The sample was rotated (4 rev/ min) during ion bombardment. Using these parameters the ion bombardment induced surface and interface morphology development generally is in the range of some nms [16].

2.2.2. Auger analysis

The exciting primary electron beam, that is, the analyzed area's diameter was 40 μm, which is less than the irradiated (ion mixed region) area, which area was at least 100x100 μm^2. Thus, it was possible to record simultaneously depth profiles on the variously intermixed and/or non-intermixed regions allowing the direct comparison of the depth profiles.

The Auger spectra were recorded by a STAIB DESA 150 pre-retarded CMA in direct current mode measuring the C, O, Si and Ga Auger peaks. The Auger peak shapes both for Si and C change due to the compound, SiC, formation as it is shown in Fig.1 (for the C region), which can be utilized to measure the SiC content as well. To do this it was assumed that the measured peak originates from carbon atoms being partly in silicon carbide state and partly graphite state. Thus, the measured peak is a simple sum of the SiC and graphite spectra. Reference Auger peaks were recorded on pure Si, graphite and nearly pure SiC (Fig. 1 shows only the peaks in the vicinity of the C peak). Using the standard spectra a simple decomposition method was used to separate the detected Auger spectrum to graphite and SiC parts. The decomposition procedure itself is a least square fitting procedure during which the best fitting intensities of the components were determined (including a background fit as well). After having the proper component peaks, the concentrations were calculated following the conventional method from the peak-to-peak amplitudes (p-p) measured on the numerically differentiated curve and applying the method of relative sensitivity factors [17].

2.2.3. *Detection of particle formation*

If the atoms form particles of size larger than 1-2 nm in diameter then the electron structure is similar to that of bulk system. Accordingly during electron irradiation plasmon losses characteristic to the material appear. These plasmon losses can be utilized for the identification

of the particles. Reflection electron energy loss spectroscopy (REELS) was used to identify the appearance of SiC and Ga particles [18].

2.3. Etching test

A typical sample contained one or more (to run several etching tests in the same time) irradiated areas of various sizes. All intermixed regions were covered by C. Thus, first we had to remove this C layer which was achieved by oxidation in microwave plasma at 500 ^{o}C.

For etching, the sample was submerged into poly-Si etchants for various times. Two types of etchants, known as possible etchant of SiC [6], were used, those of 1 unit volume HF+10.5 unit volume HNO_3+5.25 unit volume H_3PO_4 and 1 unit volume HF + 21 unit volume HNO_3, signed later as etchant *A* and *B*, respectively. The etching rates of etchants *A* and *B* are 7 and 4 μm/min measured on poly-Si, respectively. After each etching step, the surface was checked using optical microscope, which revealed the macroscopic damages and in some cases by AES depth profiling to get the depth profiles.

3. Results and discussion

3.1. The initial condition

The etching tests were carried out on the ion mixed samples. The initial condition, that is, the initial in-depth compositions of the sample was determined by AES depth profiling. A typical result is shown in Fig. 2, which shows the depth profiles after the sample was irradiated by a fluence of $40x10^{15}$ Ga^{+}/cm^{2}. Fig. 2 also shows the depth profiles of the non- irradiated sample for comparison. In the pristine sample all interfaces are sharp. Due to the irradiation serious changes occur, however. The 1st C and 1st Si layers disappear. The sample is covered by the

intermixed 1st C and 1st Si layers; concentrations vary along the depth. Besides C and Si the intermixed layer also contains Ga and SiC. The origin of Ga is evident - it is the projectile, which remains in the sample at these irradiation conditions. The appearance of SiC, which is identified by the change of the shapes of the corresponding Auger peaks (C and Si), is the result of compound formation during the intermixing process. The formation of high stability compounds at nominal room temperature during ion irradiation has been reported several times [1-5, 19]. The 2nd C, 2nd Si and 3rd C layers are unaffected by the irradiation, which is expected since the penetration (projected range) of 30 keV Ga in this layer system is 24±7 nm. We have shown that the measure of intermixing increased with fluence [15] and that majority of SiC was amorphous nano particles [18]. The intermixed layer besides SiC always contained Ga and if the fluence was $\leq$ 20 x 10^{15} Ga^+/cm^2 free (non-reacted) C and Si as well. Based on the REELS analysis, the Ga is in solution if the irradiation fluence less than 80x10^{15} Ga^+ ions/ cm^2, while it forms -at least in parts - small nanoparticles if the fluence larger than the above value [18].

The thickness of the region rich in SiC could be (arbitrarily) defined by the widths at half maximum of SiC concentration, which were found to be 7 nm, and 26 nm for fluences of 20, and 80x 10^{15} Ga^+ ions/ cm^2, respectively. It should be added, however, that the thickness of the layer is a rough measure of the SiC rich region since in the intermixed regions the depth profiles strongly vary as a function of irradiation fluence.

3.2. Chemical test

The chemical test consisted of two steps: first an oxidation in microwave plasma at 500^o C for 10 minutes was applied to remove the C (if exists) layer from the surface (later simply called as oxidation), then the sample was submerged to various etchants for various times. The non-irradiated region is used as a standard; a typical AES depth profile recorded on it after a typical

etching test (microwave oxidation + 80 s in etchant *A*) is shown in Fig. 3. The depth profile shows that the 1st C and 1st Si layers are missing. This is the expected result since the oxidation removes the 1st C layer, while 1st Si is removed by the etching (etching rate of Si for etchant *A* is 7 μm/min) in a very short, less than 1/5 s, time. The 2nd C layer is not affected by the etching, however. Fig. 4 shows the depth profiles of the irradiated area ($80x10^{15}$ Ga^+/cm^2), before and after (signed by ^{e}) the etching test which was oxidation and 80 s etching in etchant *A*. The etching test, which removed the whole 1st C and 1st Si layers from the non-irradiated region affected only a little the irradiated area; an about 5 nm thick surface layer is missing. The missing layer was made of the C not consumed by the ion mixing, implanted Ga and SiC. The atomic concentration of the SiC in the removed region was less than 20%. The free C was obviously removed by oxidation, which could not affect the SiC, which on the other hand was removed by the etching. It is important to emphasize that the etching was only effective until the SiC concentration had not exceeded about 20%. The remainder part of the sample is unchanged at the end of the etching test; the depth profiles before and after the etching test are practically the same. (The difference of the SiC distributions at 28 nm depth are most likely some experimental or evaluation error). This also means that the SiC rich intermixed region (if the SiC concentration is higher than 20%) remained on the surface safely, and protected the underlying layers, meaning that the etching rate in this region is considerably lower than that in poly-Si.

The optical microscopy image of the same surface containing the irradiated region (200x200 μm^2 region irradiated by $80x10^{15}$ Ga^+/cm^2 fluence) after oxidation and etching (80 s in etchant *A*) but before the AES depth profiling is shown in Fig. 5 suggests a more difficult picture, however. In Fig. 5 the pink square is the irradiated region. It is clear that oxidation and etching have not affected the integrity of the region, so in this respect, the optical microscopy observation agrees

with the results of the AES depth profiling. On the other hand it is evident that there are some damages on surface. It is known that the corrosion rarely attacks homogeneously the material rather it proceeds along defects e.g. phase boundaries, grain boundaries etc. In this very thin intermixed layer we cannot easily define the possible defects. Anyhow the etching definitely reveals the weak points; the total area covered by them is less than a few percentages, however. The study of these weak points etching pits, pipes, etc. which will be called as local damages, is possible by optical microscopy, while the AES depth profiling characterizes the "bulk" material. Both should be considered when describing the protection strength of the intermixed layer.

3.3. Study of macroscopic damage based on optical microscopy measurements.

In the study of macroscopic damage formation, we rely on the optical microscopy studies. Fig. 6 shows the optical microscopy image of a sample containing four 200x200 μm^2 irradiated regions; the fluences of irradiations were 10, 20, 40, 80x10^{15} Ga^+/cm^2, respectively. After oxidation (which removed the free C) the sample was immersed into etchant *B* for 24 s (in comparison, this etching would remove 1.6 μm from poly- Si). In Fig. 6 again the pink areas are the irradiated regions. The amount of defects on the four differently irradiated regions (different amounts of SiC, with different depth profiles) was different. Practically no defects were observed on the region irradiated by 80 x 10^{15} Ga^+/cm^2. Some defect could be found on the region irradiated by a fluence of 40 x 10^{15} Ga^+/cm^2. On the other hand, many local damages exhibiting a rather inhomogeneous distribution are visible on regions irradiated by fluences of 10 and 20 x 10^{15} Ga^+/cm^2. The number of local damages is clearly the highest on the region irradiated by 10 x 10^{15} Ga^+/cm^2 which contains the least amount of SiC particles. Thus, we conclude that the number of local damages produced by a given etching test depends on the amount (concentration and distribution) of SiC particles.

To estimate the resistance of the intermixed layer against the local damages as a function of layer thickness, that is, the amount of SiC particles, the sample was subjected to consecutive etching and optical microscopy observation steps until the total area of the local damages reached 5 ± 3 % of the irradiated area. The results using etchant *B* are shown in Table 1.

Based on the data of Table 1 it is clear that the time to build up the local damage depends on the thickness of the intermixed layer, but the dependence is a rather difficult one, which might be explained by the complexity of defect mediated etching processes. To characterize protection strength, we calculated the thickness which is removed under identical conditions (by applying the same etchant for the same time) from poly-Si, which will be called as "equivalent thickness". The ratio of the thickness of the intermixed layer and the corresponding equivalent thickness (shown in the 5^{th} column of Table 1) characterizes the strength of the protection as a function of the irradiation time. It is clear that the thicker the intermixed SiC rich layer (irradiation with higher fluence was used) the better the protection. In other words either the nucleation or the propagation of local defects or both are more difficult with increasing intermixed layer thickness. The extremely low numbers in the last column of Table 1 show that the protection, even in the case of the thinnest layer, is sufficiently good.

With increasing etching time the area of damaged regions increases until the integrity of the layer disappears. The result of such an experiment is shown in Fig. 7. It shows the optical microscopy images recorded on an area irradiated by $20x10^{15}$ Ga^{+}/cm^{2} after etching times of 12, 36, 60 and 84 s, using etchant *A* (etching rate for poly-Si is 7μm/min).

After 12 s of etching, some etching pits and hole like features appear. With increasing etching time the number of etching pits also increases and some of them transforms to holes (36 s). The diameter of the holes increases and after 60 s etching the intermixed layer is strongly damaged.

Further increase of the etching time results in highly non-uniform layer disappearance; after 84 s etching time only part of the intermixed layer remains.

3.4. Study of the "bulk" behavior based on AES depth profiling.

AES depth profiles were recorded on samples subjected to increasing etching times. The surprising fact is that we could not see any degradation (change of the thickness, appearance of contamination e.g. O, change of the shape of depth profiles) on the non-defective part of the irradiated region even in that case when the integrity of the intermixed layer has been lost. This is shown in Figs. 8 and 9, which show optical microscopy image and the AES depth profile of sample irradiated by fluence of $80x10^{15}$ Ga^{+}/cm^{2}, oxidized and etched for 114 s in etchant *A*. The optical microscopy image (Fig. 8) shows that part of the intermixed layer has already disappeared due to the etching and the reminder part also contains considerably amount of defective regions. On the other hand the AES depth profile, recorded on a region not showing local damage, is practically indistinguishable from the previous depth profiles shown in Fig. 4; just the surface layer containing C, Ga and less than 20% SiC is missing. Thus, the region which is non- defective is unharmed even using this heavy etching, meaning that the etching rate for non-defective intermixed region is at least 4 orders of magnitude less than that of poly-Si.

We do not know presently why the local damages appear, which actually determine the time of protection. Luckily the time required for their appearance, even in the case of the thinnest SiC rich layer intermixed region, is long enough, that is, the protection capability of the intermixed layer is sufficient. Still, if we can decrease the number of local damages, the time of protection increases by orders of magnitude.

The presented results can be explained based on the ideas reported previously [12-14,20]. First of all SiC in any form and size is highly inert and its presence reduces the effective area of the

vulnerable metallic regions, thus the presence of SiC considerably reduces the etching rate. Additionally micro-galvanic cells might form on the interfaces which strongly affect the etching rate [20]. In the present case this might be an important factor since particle/matrix interface is large as the SiC forms nanoparticles. Evidently the defects present in the surface of the intermixed region cause the formation of local damage. The propagation of these damages into the bulk is arrested by the SiC nano particles, however explaining the strong thickness dependence of the macroscopic defect formation.

4. Conclusions

Nominally C (20 nm)/Si (20nm)/ C (20 nm)/Si (20nm)/ C (20 nm)/Si substrate multilayer structure was subjected to 30 keV Ga^+ irradiation of various fluences resulting in 7-30 nm thick intermixed region containing amorphous SiC particles besides C, Si, and Ga. The actual composition and thickness of the intermixed layer depends on the fluence of irradiation. The chemical resistance of intermixed layers was tested by submerging them into different polysilicon etchants after removing the C cover layer by microwave oxidation.

The macroscopic effect of etching was studied by optical microscopy. During etching first, local damages appeared which with increasing etching time were transformed to pits, pipes and finally inhomogeneous layer removal occurred. The time for the appearance of the etching damages was high, considering the etching rate for poly-Si.

The in-depth composition of the irradiated region before and after the etching test was determined by AES depth profiling. The depth profiles measured on non-defective regions of the irradiated area did not change even during the longest etching time resulting in partial layer removal showing that the etching rate of this region is orders of magnitude less than that of poly-

Si.

References

1. M. Milosavljevic, G. Shao, N. Bibic, C.N. McKinty, C. Jeynes , K.P. Homewood, Nucl. Instrum. Methods B 188 (2002) 166-169.

2. H.F. Yan, Y.X. Shen, H. B. Guo, B X. Liu, J. Phys.:Condens. Matter 19 (2007) 026219.

3. S. Amirthapandian, B.K. Panigrahi, S. Rajagopalan , A. Gupta, K.G.M. Nair, A.K. Tyagi A. Narayanasamy, Phys. Rev. B 69 **(**2004) 165411

4. K. Nordlund, R. S. Averback Phys. Rev. B 59 (1999) 20-23.

5. G.S. Chang, S.M. Jung, J.H. Song, H.B. Kim, J.J. Woo, D.H. Byun, C.N. Whang Nucl. Instrum. Methods B 121 (1997) 244-50.

6. D. Zhuang and J.H. Edgar, Materials Science and Engineering R, 48 (2005) 1–46.

7. T. Henkel, G. Ferro, S. Nishizawa, H. Pressler, Y. Tanaka, H. Tanoue, N. Kobayashi, Mater. Sci. Forum 338 (2000) 481-484.

8. J.A. Edmond, J.W. Palmer, F Davis, J. Electrochem. Soc. 133 (1986) 650-62.

9. Fu Qian-Gang , Li He-Jun, Wang Yong-Jie, Li Ke-Zhi, Wu Heng, Ceramics International 35 (2009) 2525-2529.

10. W. Daves, A. Krauss, N. Behnel, V. Häublein, A. Bauer, L. Frey, Thin Solid Films 519 (2011) 5892–5898.

11. I. Laboriante, A. Suwandi, C. Carraro, R. Maboudian, Sensors and Actuators A 193 (2013) 238–245.

12. I. Garcia, A. Conde , G. Langelaan , J. Fransaer , J.P. Celis, Corros. Sci. 45 (2003) 1173-1189.

13. M. Lekka, N. Kouloumbi, M. Gajo, P.L. Bonora, Electrochim. Acta 50 (2005) 4551–4556.

14. B. Bakhit, A. Akbari, Surf. Coat. Technol. 206 (2012) 4964–4975.

15. Á. Barna, S. Gurban, L. Kotis, J. Lábár, A. Sulyok, A. L. Tóth, M. Menyhárd, J. Kovac, P. Panjan, Appl. Surf. Sci. 263 (2012) 367 –372.

16. M. Menyhard, Micron 30 (1999) 255–265.

17. *Handbook of Auger Electron Spectroscopy*, *Third Edition*, 1995 Eds. K.D. Childs, B.A. Carlson, L.A. LaVanier, J.F. Moulder, D.F. Paul, W.F. Stickle, D.G. Watson , Eden Prairie, Minnesota.

18. M. Menyhard , J. Phys D: Appl. Phys. 46 (2013) 415304.

19. Ram Prakash, S. Amirthapandian, D.M. Phase, S.K. Deshande, R. Kesavamoorthy, K.G.M. Nair, Nucl. Instrum. Methods Phys. Res. B 244 (2006) 283-288.

20. X.H. Chen, C.S. Chen, H.N. Xiao, F.Q. Cheng, G. Zhang, G.J. Yi, Surf. Coat. Technol. 191 (2005) 351–356.

Figure captions

1. Decomposition of the measured Auger spectrum in the vicinity of the carbon line for graphitic and silicon carbide parts. The standard spectra were recorded on pure graphite and SiC, respectively. The components heights were determined by linear best fitting of reference spectra.
2. The depth profiles determined by AES depth profiling on the pristine sample, and on the region irradiated by fluence of 40 x 10^{15} Ga^{+}/cm^{2}.
3. The AES depth profile recorded on the non-irradiated sample after etching test (microwave oxidation, 80 s etching in etchant *A*) .
4. Depth profiles measured on irradiated ($80x10^{15}$ Ga^{+}/cm^{2}) region before (Si, C, SiC, Ga) and after (Si^{e}, C^{e}, SiC^{e}, Ga^{e}) the etching test, which was oxidation and 80 s etching in etchant *A*.
5. The optical microscopy image of the irradiated region ($80x10^{15}$ Ga^{+}/cm^{2}) after oxidation and 80 s etching in etchant *A*.
6. The optical microscopy image of a sample irradiated on four (200x200 μm^{2}) regions applying 10, 20, 40, $80x10^{15}$ Ga^{+}/cm^{2} fluences, then oxidized and finally etched in etchant *B* for 24s.
7. The optical microscopy images taken from an irradiated ($20x10^{15}$ Ga^{+}/cm^{2}) regions after oxidation and etching (etchant *B*) for 12s *a*, 36s *b*, 60 s *c*, 84 s *d*.
8. The optical microscopy image of irradiated ($80x10^{15}$ Ga^{+}/cm^{2}) region after microwave oxidation and etching in etchant *A* for 114 s.
9. The AES depth profile recorded on the "non-defective" part of irradiated region shown in Fig. 8.

Table 1

Irradiation fluence (10^{15} Ga^{+}/cm^{2})	Thickness of SiC rich layer (nm)	Time to reach 5% dam. area (s)	Equivalent thickness (nm)	Ratio of columns 2 and 4
10	8	5	300	0.026
20	17	18	1200	0.014
40	31	55	3500	0.02
80	26	110	7300	0.004

The thickness dependence of the formation of local damages. Columns 1-3 show the fluence of irradiation used to make the intermixed layer, the thicknesses of the intermixed layers, and the etching times (using etchant *B*) necessary to produce 5±3% coverage of local damages. Column 4 gives the thicknesses of poly-Si which is removed during the times given in column 3. The last column gives the ratios of thickness values being in column 2 and 4.

Figures

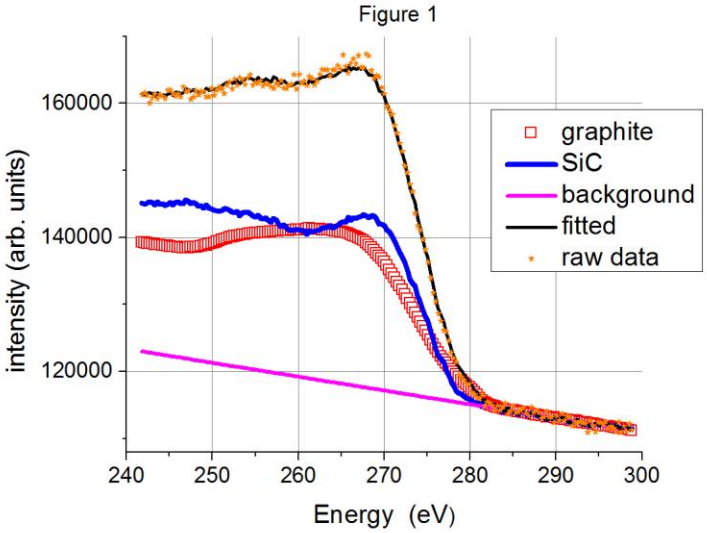

Figure 1

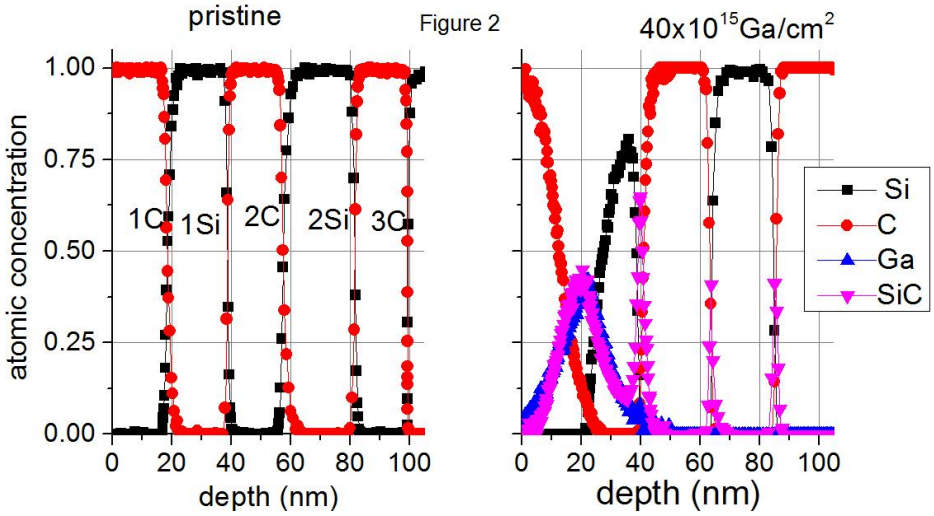

Figure 2.

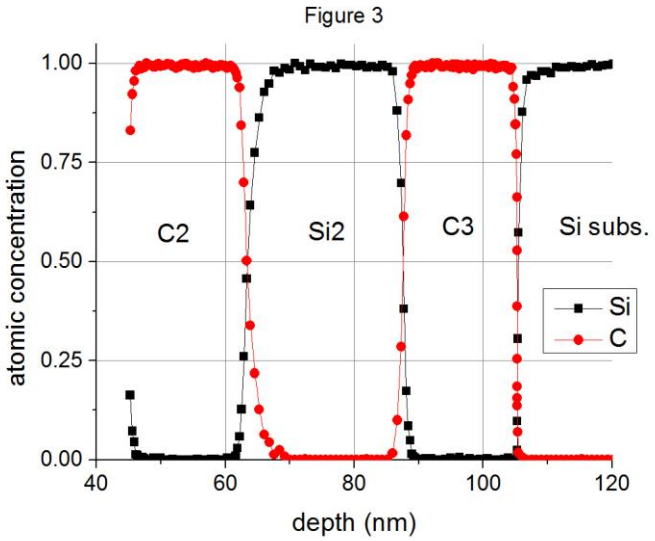

Figure 3.

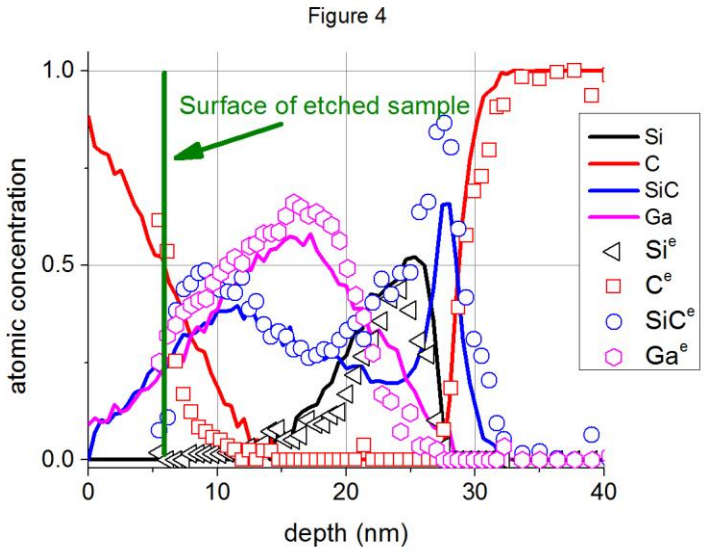

Figure 4.

Figure 5

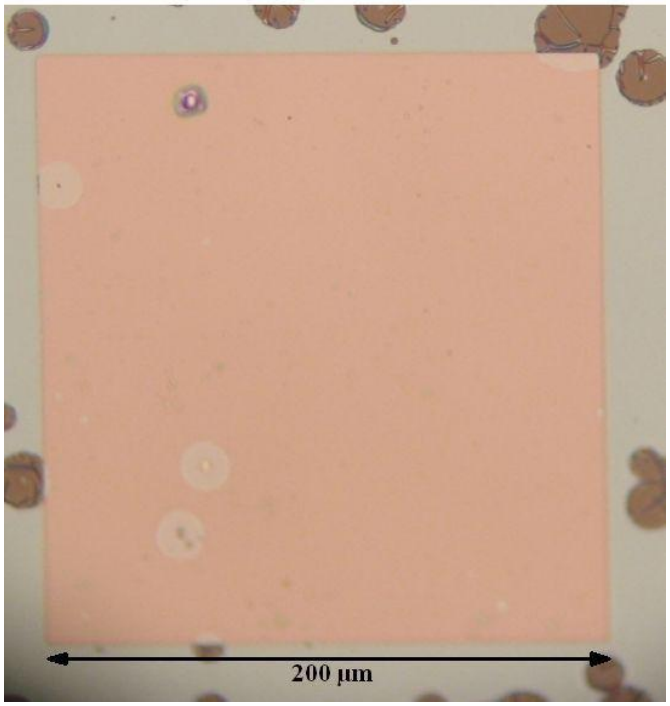

Figure 5.

Figure 6

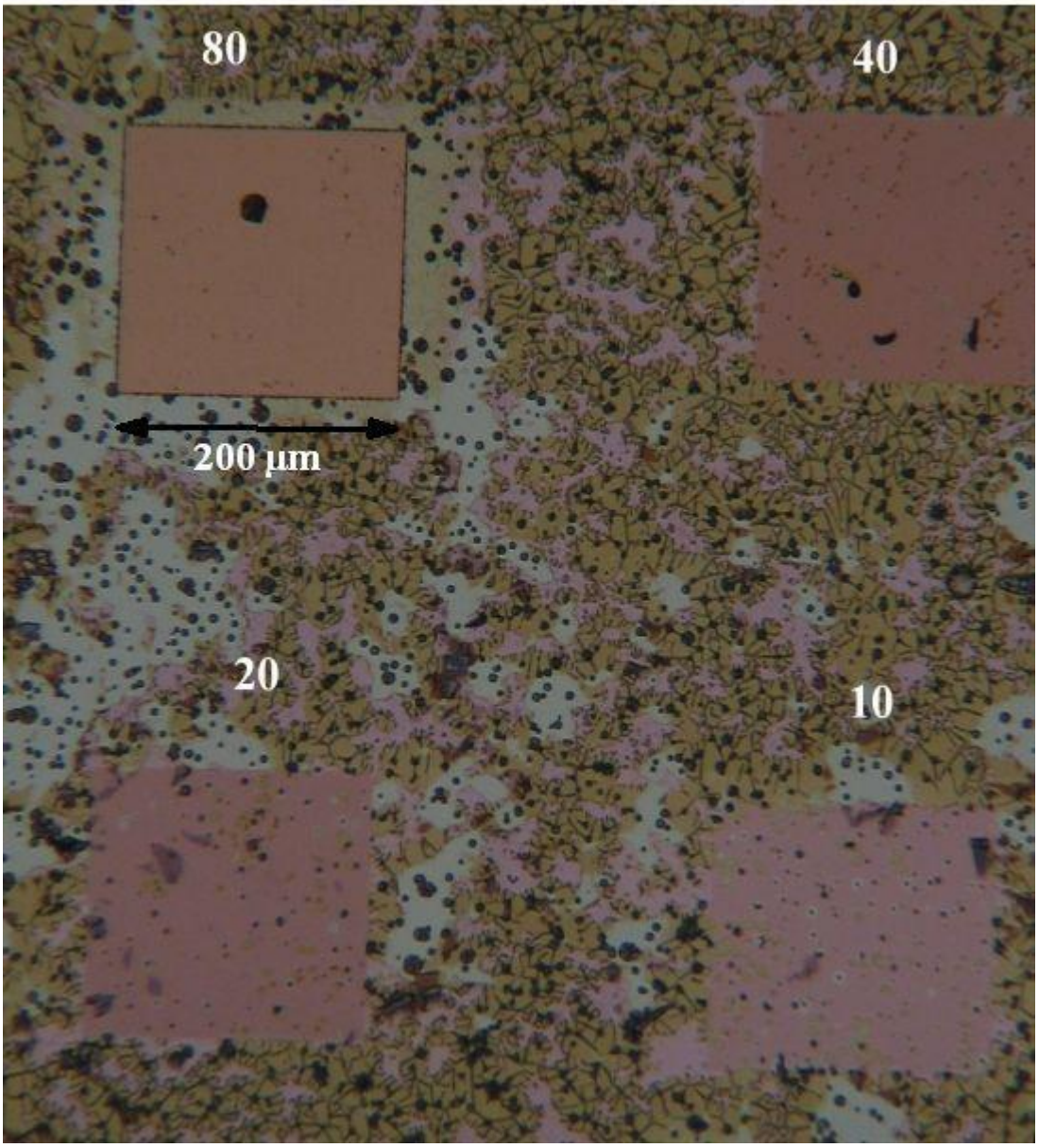

Figure 6.

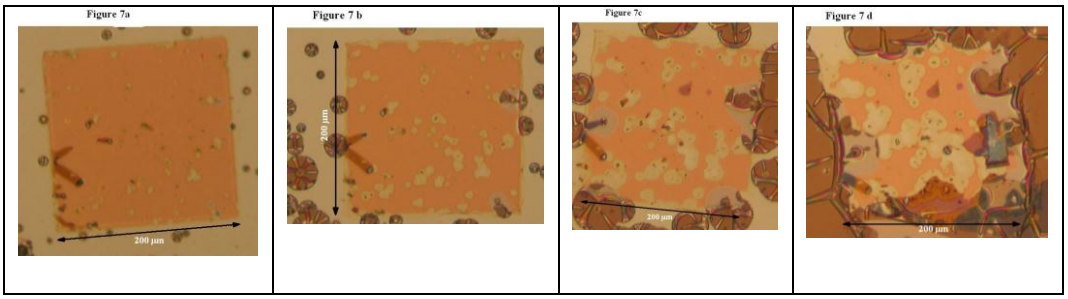

Figure 7a Figure 7b Figure 7c Figure 7d

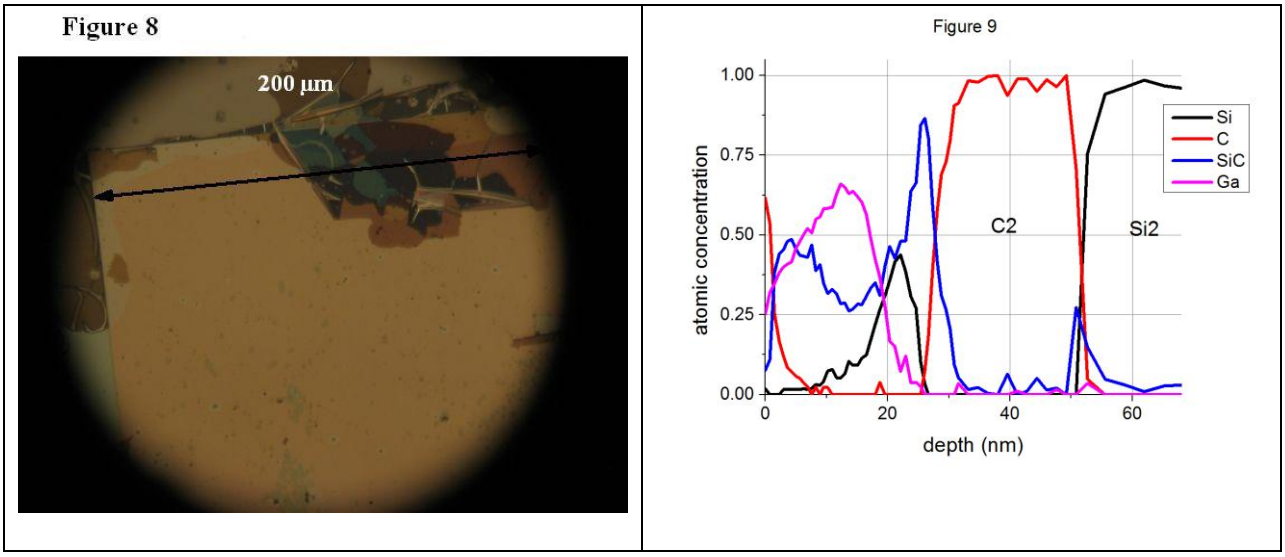

Figure 8. Figure 9.